## 8.5 RECENT PROGRESS IN TIDAL MODELING

## F. Vial

Laboratoire de Meteorologie Dynamique du CNRS Ecole Polytechnique, 91128 Palaiseau Cedex, France

## J. M. Forbes

College of Engineering, Boston University 110 Cummington Street, Boston, MA 02215

Recent contributions to tidal theory during the last five years are reviewed. Specific areas where recent progress has occurred include: the action of mean wind and dissipation on tides, interactions of other waves with tides, the use of TGCM in tidal studies. Furthermore, attention is put on the nonlinear interaction between semidiurnal and diurnal tides. Finally, more realistic thermal excitation and background wind and temperature models have been developed in the past few years. This has led to new month-to-month numerical simulations of the semidiurnal tide. Some results using these models are presented and compared with ATMAP tidal climatologies.

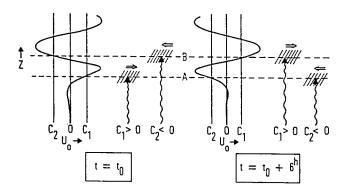


Figure 1. Schematic representation of modulation of wave-mean flow interaction by imposed tidal oscillation.  $U_0$  represents the tidal velocity,  $c_1$  and  $c_2$  the phase velocities of the two waves whose upward propagation is denoted by the wavy lines. The hatched areas indicate regions where the waves are significantly absorbed. The open arrows indicate the sense of the acceleration induced by absorption [Walterscheid, J. Geophys. Res., 86, 9698 1981].

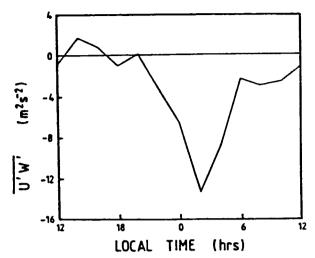


Figure 2. Mean momentum flux as a function of local time as measured with an MF radar at Adelaide (35°) during the 9 - 17 June 1984 period [Fritts and Vincent, *J. Atmos. Sci.*, 44, 605, 1987].

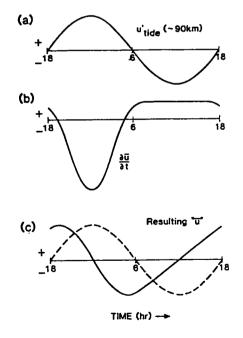


Figure 3. Schematic illustrating the effects of diurnally varying zonal drag on the inferred tidal structure. The results are an altered amplitude and an advanced phase of the apparent tidal motion [Fritts and Vincent, *J. Atmos. Sci.*, 44, 605, 1987].

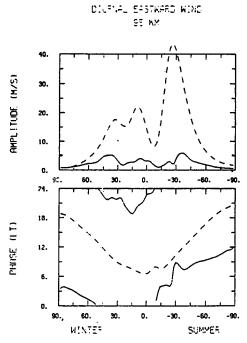


Figure 4. Comparison of the latitudinal structure of amplitude and phase of solar-driven (solid line) and nonlinear (dashed line) diurnal tides at 95 km for solstices conditions [H. Teitelbaum et al., private communication].

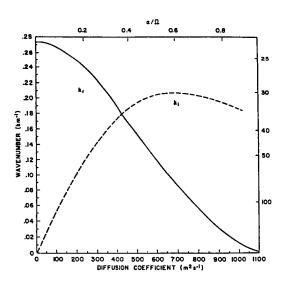
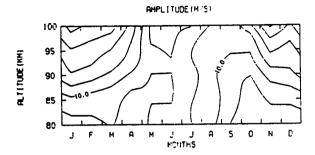


Figure 5. Real and imaginary part of the diurnal tide vertical wave number plotted as a function of eddy diffusion  $K_{zz}$ , and equivalently as a function of the Rayleigh friction coefficient  $\alpha$  normalized to the earth rotation rate  $\Omega$  [Forbes and Vincent, Planet. Space Sci., 1988, in press].

EASTHARD WIND

LAT=44 N





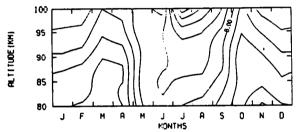
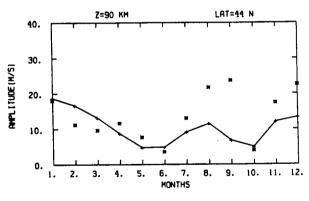


Figure 6. Height vs month contour of amplitude and phase structures at 44° N obtained from monthly simulations of the semidiurnal tide. Contours are plotted with steps of 5 m/s and 1 hour, respectively [Forbes and Vial, 1988, this volume].





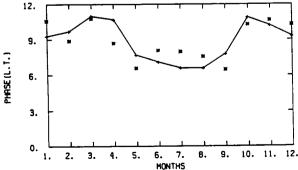


Figure 7. Semidiurnal modeled amplitude and phase at 90 km and 44° N obtained from monthly simulations of the semidiurnal tide. Comparisons are made with monthly tidal climatology data from Monpazier (44°N) [Forbes and Vial, 1988, this volume].